Limiting forms for capillary–gravity waves

By M. S. LONGUET-HIGGINS

Department of Applied Mathematics and Theoretical Physics, University of Cambridge,
Silver Street, Cambridge, CB3 9EW, UK *and* Institute of Oceanographic Sciences, Wormley,
Surrey, UK

The form of steep capillary waves is of interest as a possible initial condition for the formation of air bubbles at a free surface. In this paper the limiting forms of pure capillary waves and of quasi-capillary waves are studied analytically. Crapper's finite-amplitude solution is expressed in a simple form, and is shown to be one of several exact elementary solutions to the pure-capillary free-surface condition. Among others are the solution $z = w + \sinh w$, where w is the velocity potential, and also $z = w^3$. The latter solution, though it represents a self-intersecting flow, can be used as the first in a sequence of approximations to the form of the steepest wave. Hence it is shown that the influence of gravity on the shape of the limiting 'bubble' is very small. The result is confirmed by an examination of Hogan's numerical calculations of limiting capillary–gravity waves.

In the crest of a limiting wave the particle velocity is almost constant and equal to the phase speed. This property makes it possible to apply a quasi-static approximation so as to determine the form of the crest, and hence to find an expression for the complete profile of a capillary–gravity wave of limiting steepness. It appears that there exists a solitary wave of capillary–gravity type on deep water.

1. Introduction

While much attention has been given recently to the limiting forms of steep gravity waves, and the way in which such waves may overturn and trap air bubbles at the sea surface, rather few studies have been made of steep capillary or gravity–capillary waves. Yet this subject may be of considerable interest not only on account of its relevance to the exchange of gasses and water droplets between the atmosphere and ocean, but also on account of the probable contribution to the underwater acoustical background made during the process of bubble formation.†

Long after Wilton's (1915) pioneering study of nonlinear gravity–capillary waves, the most striking and surprising addition to the literature came with Crapper's (1957) discovery of an exact solution to the problem of pure capillary waves on water of infinite depth. This showed that, as the wave steepness increases, so the wave crests become more flat and the troughs become more curved (the complete opposite of pure gravity waves), until the free surface in the trough becomes vertical and then finally touches itself, pinching off a bubble of 'air'. This prediction has received experimental support from laboratory studies by Schooley (1958).

† See the Proceedings of the NATO Workshop on Natural Mechanisms of Surface Generated Noise in the Ocean, held at Lerici, Italy, from 15–19 June 1987.

A corresponding exact solution for water of finite depth, also mentioned by Crapper (1957), was worked out in detail by Kinnersley (1976). The solution, which is in terms of elliptic functions, is applicable also to symmetric waves on a thin sheet of fluid. Kinnersley obtained also the corresponding antisymmetric solutions, thus generalizing to waves of finite amplitude the theory accompanying Taylor's (1959) elegant experiments on thin sheets of fluid.

For gravity–capillary waves no exact solutions are known, but precise numerical calculations have been carried out by Hogan (1980) which show that in one class of gravity–capillary waves (which we shall call the 'quasi-capillary' waves) a similar phenomenon occurs, in which the free surface touches itself, thereby trapping a bubble of air. In such an event, of course, the surface would in practice immediately shorten and adjust itself so as to reduce the surface-tension energy. Hence this type of limiting configuration can exist only for a fleeting instant,† in contrast to the situation for pure gravity waves, where the Stokes 120° corner flow is a theoretically possible steady flow, even though it may in fact be unstable.

The purpose of the present paper is to study the form of the final 'pinch', at the instant when the surface touches itself, as an initial condition for the formation of the bubble and the generation of a pulse of sound when it breaks away from the free surface. In this process, because of the short timescales involved, gravity is unlikely to have much *direct* influence, and capillarity is all-important.

In §2 the capillary surface condition is first expressed in a convenient form, and in §§3–7 we note the existence of several exact solutions in terms of elementary functions: the circular vortex (§3); a hyperbolic or catenary flow (§4); the Crapper surface wave, expressed in simple form (§5); a flow possibly relevant to a steady jet impinging on a flat fluid surface (§6); and a simple cubical flow (§7). The last two both involve self-intersecting streamlines, but it is pointed out that the latter, in particular, is of use mathematically as the first term in a sequence of approximations to realizable physical flows (see §8). This enables us to estimate, in §9, the influence of gravity on the form of the limiting 'bubble', and to show that it is indeed small. The result is confirmed by examination of Hogan's (1980) accurate computation of the surface profiles.

In the wave crest, on the other hand, the particle velocities relative to the phase speed are shown to be small, with the result that one may apply a quasi-static approximation and obtain an expression for the surface profile in terms of known functions (§11). In this expression, as the wavelength tends to infinity, the depth of the bubble 'neck' remains bounded, yielding a solitary wave (on deep water) with calculable properties (§12). The 'bubble' size is determined by the radius of curvature at the 'neck', which is also finite.

In §13 we estimate the phase speed both of the solitary wave and of the more general periodic wave of limiting steepness, and in §14 we note a small correction to the crest profile so as to take account of the non-zero particle velocity. The maximum bubble diameter arising from detached wave troughs is calculated in §15 and is shown to be consistent with the laboratory experiments of Schooley (1958). A discussion follows in §16, and the conclusions are summarized in §17.

† For this reason a class of steady flows calculated numerically by Vanden-Broeck & Keller (1980), in which the pressure in the 'bubble' differs from that at the free surface, seems to have little applicability.

2. The free-surface condition

Consider a frictionless, incompressible fluid, of uniform density, in steady irrotational motion. Let $z = x + iy$ denote a complex Cartesian coordinate and $w = \phi + i\psi$ the complex velocity potential. The vector fluid velocity is given by

$$w_z^* = q\,e^{i\theta}, \tag{2.1}$$

q being the magnitude and θ the direction of the flow (an asterisk denotes the complex conjugate). Hence also

$$z_w = q^{-1}\,e^{i\theta} \tag{2.2}$$

and we see that

$$\theta + i\ln q = -i\ln z_w \tag{2.3}$$

is an analytic function of z or of w.

The boundary condition on a free streamline ($\psi = \text{constant}$) is

$$p + \tfrac{1}{2}q^2 + T\kappa + gy = \text{constant}, \tag{2.4}$$

where p denotes the pressure, T and q surface tension and gravity respectively, and κ is the curvature. The coordinate y is measured vertically upwards. We seek to express (2.4) in a form such that w is the independent and z the dependent variable. Now if s denotes the arc length along any given streamline we have

$$-\kappa = \frac{d\theta}{ds} = \frac{d\phi}{ds}\frac{d\theta}{d\phi} = q\,Re\,\frac{d(\theta + i\ln q)}{dw}. \tag{2.5}$$

By equation (2.3) this is

$$\kappa = \tfrac{1}{2}iq\left(\frac{z_{ww}}{z_w} - \frac{z_{ww}^*}{z_w^*}\right). \tag{2.6}$$

We have also

$$q^{-2} = z_w z_w^*. \tag{2.7}$$

So the condition (2.4) becomes

$$2p + q^2 + iTq\left(\frac{z_{ww}}{z_w} - \frac{z_{ww}^*}{z_w}\right) - ig(z - z^*) = \text{constant}, \tag{2.8}$$

where q is given by (2.7).

In the case when the pressure is assumed constant and gravity is negligible, equation (2.8) reduces to

$$q^2 + iT\left(\frac{z_{ww}}{z_w} - \frac{z_{ww}^*}{z_w^*}\right) = \text{constant}. \tag{2.9}$$

We shall now discuss some exact, elementary solutions of (2.9). For the sake of simplicity we choose lengthscales so as to give convenient expressions; conversion to other units is straightforward.
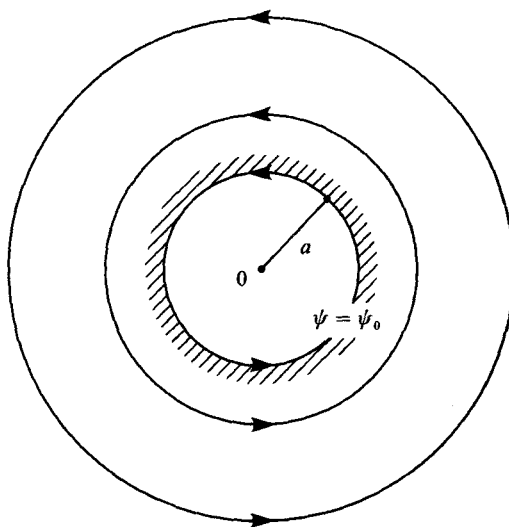
3. $z = e^{iw}$

This represents a simple vortex; see figure 1. From (2.6) and (2.7) we have

$$-\kappa = q = e^\psi \tag{3.1}$$

so that (2.8) yields

$$e^{2\psi} - 2T\,e^\psi = \text{constant}. \tag{3.2}$$

The condition can be satisfied on any circular streamline, having radius $a = e^{-\psi}$. If p_0 denotes the pressure on the free surface ($\psi = \psi_0$) and p_∞ the pressure at infinity

M. S. Longuet-Higgins

FIGURE 1. The circular vortex $z = e^{iw}$.

$(\psi = -\infty)$ the constant on the right of (3.2) is $2(p_0 - p_\infty)$. In particular if $p_0 = p_\infty$ we obtain

$$T = \tfrac{1}{2}\, e^{\psi} = \frac{1}{2a}. \tag{3.3}$$

In other words, the greater the surface tension, for a vortex of fixed strength, the smaller the bubble diameter.

4. $z = w + \sinh w$

On differentiating, we have

$$z_w = 1 + \cosh w = 2 \cosh^2 \tfrac{1}{2}w, \tag{4.1}$$

a perfect square, so that from (2.7)

$$q^{-1} = 2 \cosh \tfrac{1}{2}w \, \cosh \tfrac{1}{2}w^*. \tag{4.2}$$

Moreover

$$\frac{z_{ww}}{z_w} = \tanh \tfrac{1}{2}w \tag{4.3}$$

and so from (2.5)

$$\kappa = \frac{\sinh \psi}{2 \cosh^2 \tfrac{1}{2}w \, \cosh^2 \tfrac{1}{2}w^*}. \tag{4.4}$$
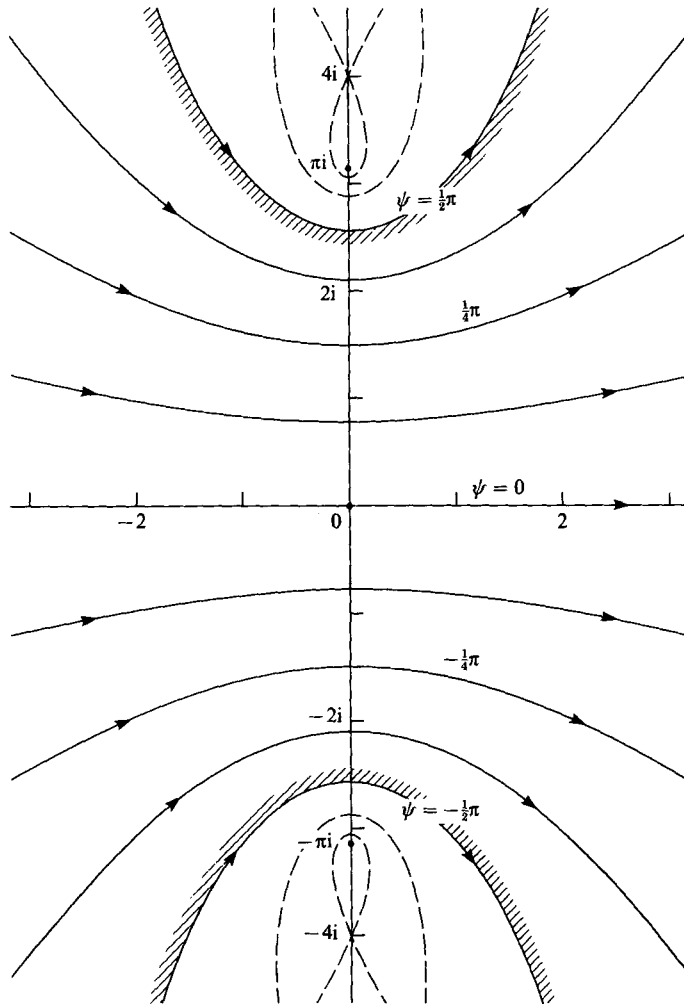
So (2.9) is satisfied on $\psi = \psi_0$ provided that

$$1 + 2T \sinh \psi_0 = 0 \tag{4.5}$$

or

$$T = \frac{-1}{2 \sinh \psi_0}. \tag{4.6}$$

The streamlines are given parametrically by

$$\left. \begin{array}{l} x = \phi + \cos \psi \, \sinh \phi, \\ y = \psi + \sin \psi \, \cosh \phi \end{array} \right\} \tag{4.7}$$

FIGURE 2. Streamlines of the flow $z = w + \sinh w$.

and are shown in figure 2. The flow is symmetric about the x-axis ($\psi = 0$), and provided $|\psi| < \frac{1}{2}\pi$ the asymptotes make angles $\pm \psi$ with the x-axis. When $\psi = \frac{1}{2}\pi$ the streamline is the catenary

$$y = \tfrac{1}{2}\pi + \cosh x. \tag{4.8}$$

When $|\psi| > \frac{1}{2}\pi$ the streamlines are self-intersecting at the point given by

$$\frac{\sinh \phi}{\phi} = -\cos \psi \tag{4.9}$$

and the solution is non-physical, if considered in the entire plane.

Clearly the streamline $\psi = 0$ may be replaced by a plane boundary (friction being neglected). In fact the flow will be seen to be identical with a limiting form of finite-amplitude capillary waves derived by Kinnersley (1976, equation (72)) for water of finite depth.

5. $z = w - \tan w$

This is Crapper's deep-water capillary wave (Crapper 1957) thrown into its simplest form. Clearly we have

$$z_w = 1 - \sec^2 w = -\tan^2 w, \tag{5.1}$$

again a perfect square, giving

$$q^{-1} = \tan w \tan w^* \tag{5.2}$$

and

$$\frac{z_{ww}}{z_w} = \frac{2}{\sin w \cos w}. \tag{5.3}$$

Hence

$$\kappa = \frac{\cos 2\phi \sinh 2\psi}{\sin^2 w \sin^2 w^*} \tag{5.4}$$

and

$$q^2 - 1 = \frac{\cos 2\phi \cosh 2\psi}{\sin^2 w \sin^2 w^*} \tag{5.5}$$

so that the boundary condition (2.8) is satisfied on $\psi = \psi_0$ provided only that

$$T = -\tfrac{1}{2} \coth 2\psi_0. \tag{5.6}$$

It will be noted that ψ_0 is generally negative.

The above solution was expressed by Crapper (1957) in terms of a parameter

$$A \sim e^{2\psi_0} \tag{5.7}$$

so that the dispersion relation (5.6), for example, becomes

$$\frac{kT}{c^2} = \frac{1 + A^2}{1 - A^2} \tag{5.8}$$

in dimensional form. Here k and c denote the wavenumber ($= 2\pi/\text{wavelength}$) and the phase speed, respectively. In the solution (5.1) we have $k = 2$ and $c = 1$.

The form of the streamlines $\psi = $ constant are shown in figure 3. They clearly correspond to a wave of finite amplitude, as seen in a reference frame moving with the phase speed. Any streamline $\psi = \psi_0$ may be taken as the free surface provided $\psi_0 \geqslant \psi_{\text{crit}} = -0.394$ (that is $A \leqslant 0.455$). The critical streamline $\psi = \psi_{\text{crit}}$ touches itself, enclosing a 'bubble'.

However, when $\psi_0 < \psi_{\text{crit}}$ the surface intersects itself and the flow becomes multivalued (see figure 4). Flows in this range have usually been ignored as being unphysical. Nevertheless they turn out to be of some use mathematically as we shall see below in §8.

Here we note that as $\psi_0 \to 0$ and $w \to 0$ the asymptotic behaviour of the flow is given by

$$z = w - \tan w \sim -\tfrac{1}{3} w^3. \tag{5.9}$$

On the other hand as $\psi_0 \to 0$ but $w \to \tfrac{1}{2}\pi$ we have

$$z = w + \cot (w - \tfrac{1}{2}\pi) \sim \tfrac{1}{2}\pi + \frac{1}{w - \tfrac{1}{2}\pi}, \tag{5.10}$$
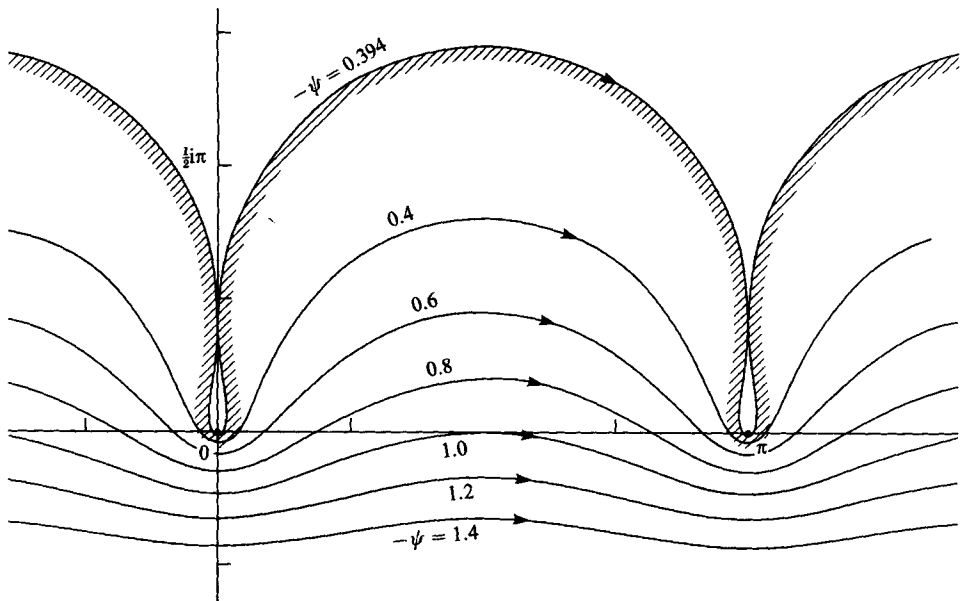
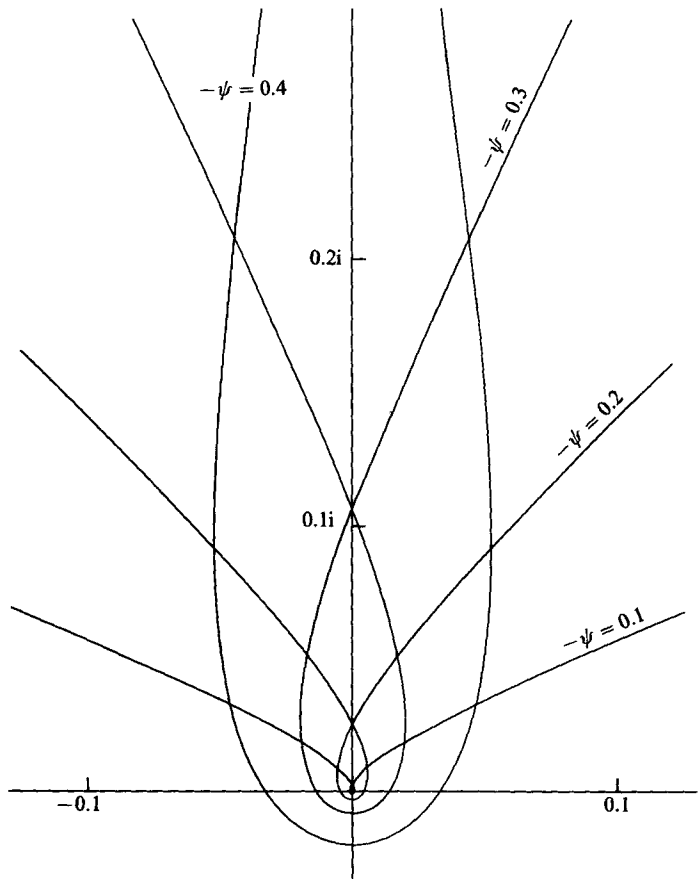FIGURE 3. Streamlines of the flow $z = w - \tan w$, representing a pure capillary wave on deep water.

FIGURE 4. Streamlines for $z = w - \tan w$ near the origin, when ψ_0 is small.
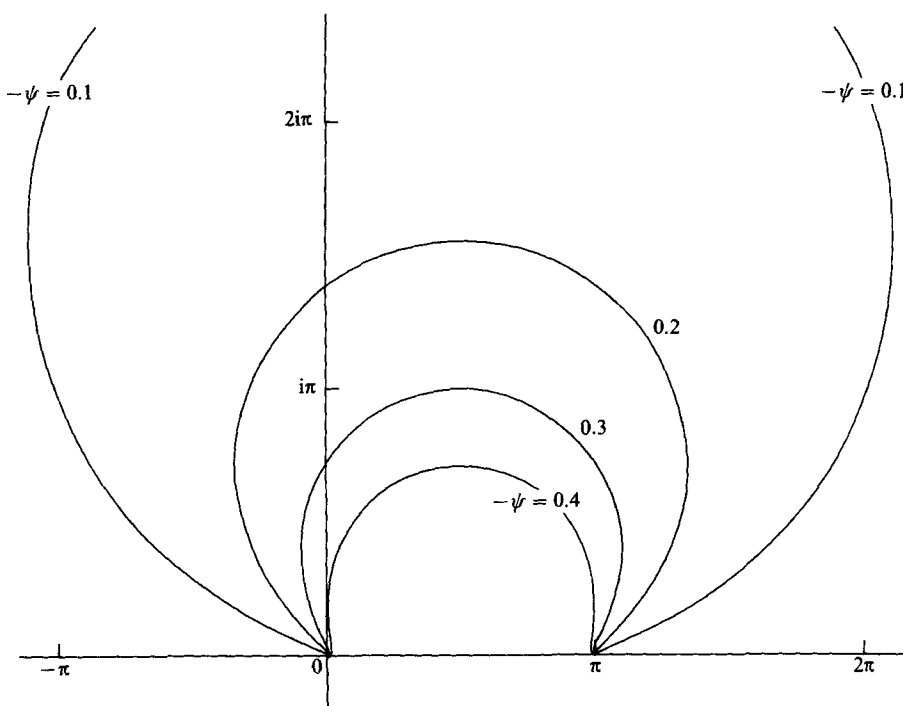
FIGURE 5. Streamlines for $z = w - \tan w$ near the point $w = \frac{1}{2}\pi$, when ψ_0 is small.

the flow being dominated by the pole at $w = \frac{1}{2}\pi$. The corresponding part of the free surface is thus almost circular, as seen in figure 5. The square of the velocity is given by

$$q^2 \sim |w - \tfrac{1}{2}\pi|^4 \tag{5.11}$$

which is very small, making the curvature κ almost constant; the free surface is like an almost stationary cylindrical balloon.

6. $z = w + \sin w$ and $z = w - \tanh w$

For the sake of completeness we mention here two solutions which are related to those discussed in §§4 and 5, respectively. The first,

$$z = w + \sin w, \tag{6.1}$$

will be found to satisfy the boundary condition (2.9) on $\psi = \psi_0$ provided only that

$$T = -\frac{1}{2 \sinh \psi_0}. \tag{6.2}$$

The second,
$$z = w - \tanh w, \tag{6.3}$$

satisfies (2.9) provided that
$$T = -\tfrac{1}{2} \cot 2\psi_0. \tag{6.4}$$

In both cases the streamlines are self-intersecting, as seen in figures 6 and 7 respectively. However, while the flow (6.1) is extremely multivalued, it is quite conceivable that if (6.3) were modified by the inclusion of gravity it could correspond to the flow of a jet impinging on a plane water surface.
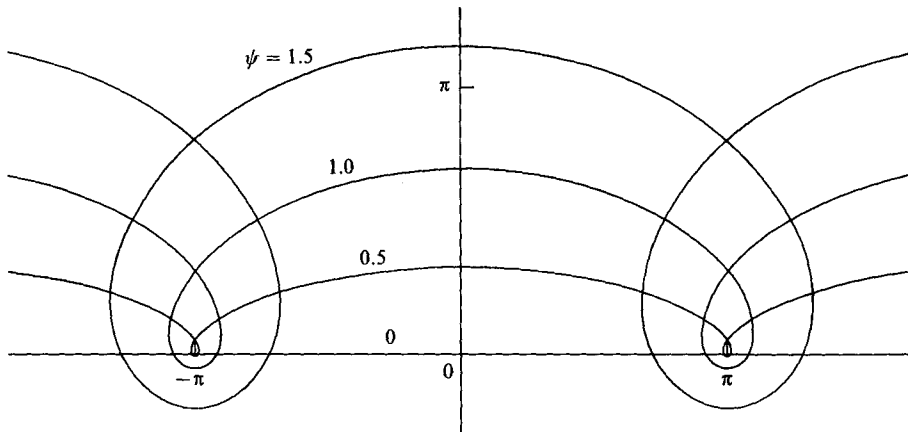
FIGURE 6. Streamlines of $z = w + \sin w$.
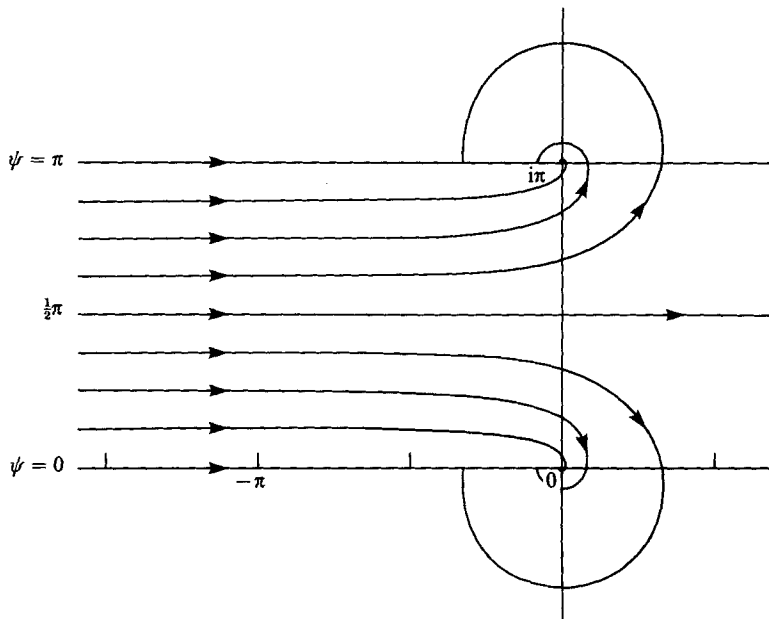

FIGURE 7. Streamlines of $z = w - \tanh w$.

7. $z = \frac{1}{3}w^3$

This simple expression, which has already been seen to be a local limiting form of the flow described in §5, turns out to be itself an exact solution to the boundary conditions. For we have

$$z_w = w^2, \tag{7.1}$$

hence

$$q = \frac{1}{ww^*} \tag{7.2}$$

and

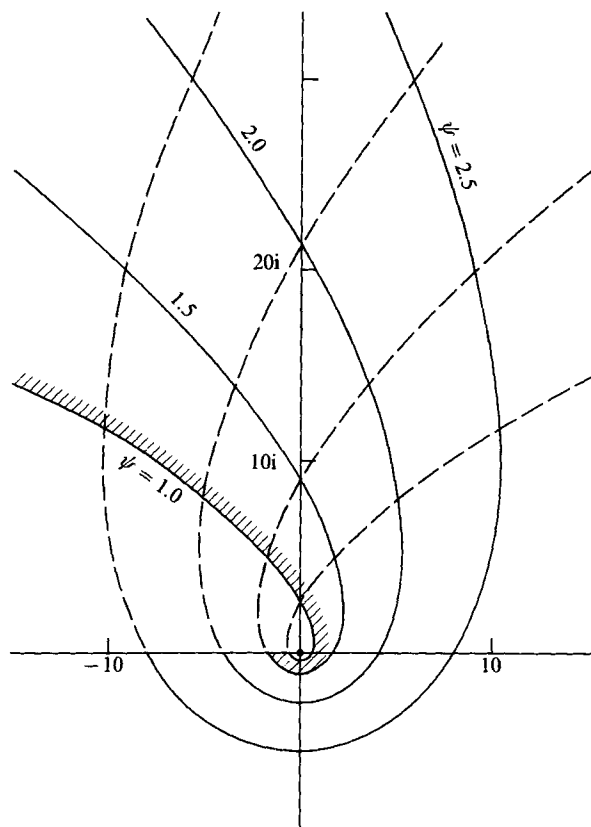$$\kappa = \frac{2\psi}{(ww^*)^2}. \tag{7.3}$$

FIGURE 8. Streamlines of $z = \frac{1}{3}w^3$.

Therefore equation (2.8) is satisfied on $\psi = \psi_0$ provided

$$T = -\frac{1}{4\psi_0}. \tag{7.4}$$

The streamlines, shown in figure 8, are all self-similar and self-intersecting, so that the overall flow is not physical. We shall see, however, that the solution is useful as a first approximation to the initial form of an entrained bubble.

We note that the corresponding 'dipole' expression

$$z = w^{-1}, \tag{7.5}$$

which also occurs as an asymptotic form in §5, and which also gives a squared expression for z_w, is nevertheless not an exact solution of the boundary condition.†

8. Higher approximations

With a view to studying the effect of gravity on the 'loop' enclosed by a steep wave we consider first some higher approximations to the form of the loop, based on expansions, not for $A \ll 1$, as in the small-amplitude approximation of Stokes or Wilton, but about $w = 0$ ($A = 1$).

† The solution $z = \frac{1}{3}w^3$ can also be derived from equations (40) and (41) of Crapper (1957) on setting $a_2 = a_3 = 0$.
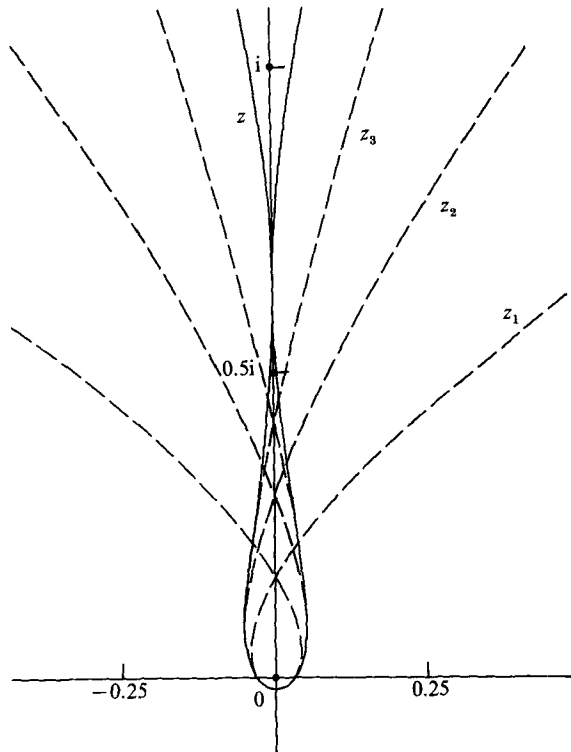
FIGURE 9. Successive approximations to the limiting 'bubble', corresponding to partial sums in the series (8.1).

Thus to order w^7, say, we have from §5

$$z = w - \tan w$$
$$= -\tfrac{1}{3}w^3 - \tfrac{2}{15}w^5 - \tfrac{17}{315}w^7 - \dots \qquad (8.1)$$

(see Abramowitz & Stegun 1965, p. 75). The lowest-order approximation, which is exact, was studied in the previous Section. The next approximation

$$z = -\tfrac{1}{3}w^3 - \tfrac{2}{15}w^5, \qquad (8.2)$$

is not an exact solution, but will be found to satisfy the boundary conditions to order ψ_0^3 provided that

$$T = -\frac{1}{2}\left(\frac{1}{2\psi_0} + \frac{2\psi_0}{3}\right). \qquad (8.3)$$

Similarly the next approximation satisfies the boundary condition to order ψ_0^5 provided that

$$T = -\frac{1}{2}\left(\frac{1}{2\psi_0} + \frac{2\psi_0}{3} - \frac{8\psi_0^3}{45}\right), \qquad (8.4)$$

the last two equations representing successive partial sums in the expansion of $-\tfrac{1}{2}\coth 2\psi_0$ in powers of ψ_0.

Figure 9 shows the first three approximants to the surface profile in the critical case $\psi_0 = -0.394$.

K	H/L	$R = \delta/L$	$r = \delta/h$
∞	0.7298	0.316	0.149
10	.5560	.0199	.151
5	.4726	.0156	.152
1	.2569	.0074	.154

TABLE 1. Parameters of capillary–gravity waves

The series (8.1) has a radius of convergence $|w| = \frac{1}{2}\omega$ (corresponding to the nearest pole of $\tan w$) and so is convergent when $|\phi| < (\frac{1}{4}\pi^2 - \psi_0^2)^{\frac{1}{2}} = 1.521$. The value of $|\phi|$ at the point of contact is only 1.024.

9. The effect of gravity

In the boundary condition (2.7) the term involving gravity g is, to lowest order,

$$-ig(z - z^*) = \tfrac{1}{3}ig(w^{*3} - w^3)$$
$$= \tfrac{2}{39}g\psi_0(3\phi^2 - \psi_0^2). \tag{9.1}$$

This compares with the terms $(q^2 - 1)$ and $T\kappa$ which are of order T/ψ_0^3. We therefore expect that gravity will have an effect at order ψ_0^3 and that its relative magnitude will be of order $g\psi_0^6/T$. In dimensional terms this is

$$(g/Tk^2) \times (\psi_0 k/c)^6. \tag{9.2}$$

For gravity–capillary waves, in which (g/Tk^2) is of order 1, and where $\psi_0 k/c$ is of order $\frac{2}{3}$ or less, we expect effects of order 10^{-1} at most.

Hogan (1980, 1981) has calculated numerically the profiles of steep gravity–capillary waves for values of the parameter

$$K = Tk^2/g \tag{9.3}$$

ranging from $\frac{1}{2}$ to ∞. Measurements of the critical profiles shown in figure 12 of Hogan (1981)† are summarized in table 1 below. R denotes the ratio of the bubble width δ to the wavelength L of the wave, and r denotes the 'aspect ratio' δ/h of the bubble, h being the vertical distance between the 'neck' of the bubble and the lowest point on the profile. H is the total crest-to-trough wave height. It will be seen that while R varies over a range of almost 4 to 1, the aspect ratio r varies only between 0.149 and 0.154.

Hogan (1981) has also drawn profiles for the case $K = 0.5$ but these are thought to be less accurate owing to incomplete convergence of the Padé approximants (see Hogan 1981, p. 408).

10. Form of the crest in a capillary–gravity wave

It was Wilton (1915) who first showed that for a given wavelength it may be possible for more than one type of capillary–gravity wave to exist. For simplicity we shall limit discussion initially to the waves denoted as Type 1 in the numerical computations by Schwartz & Vanden-Broeck (1979).‡

† Dr Hogan kindly supplied the original calculations on which his profiles are based.
‡ See also Chen & Saffman (1979, 1980).

As shown above in §5, and mentioned also by Crapper (1957) the particle velocity q in the upper half of a pure capillary wave ($K = \infty$) is very small, leading to an almost circular profile for the wave crest. We suspect that the same may be true also for the more general capillary–gravity waves (K finite) when these are steep enough to develop a high curvature in the wave troughs.

Let us then assume the square of the velocity q to be negligible, so that the boundary condition (2.4) becomes, when $p = 0$,

$$T\kappa + gy = \text{constant.} \tag{10.1}$$

For simplicity we shall choose units so that

$$T = g = 1 \tag{10.2}$$

(so that in dimensional terms the units of length and velocity are respectively $(T/g)^{\frac{1}{2}}$ and $(gT)^{\frac{1}{4}}$). Then if α denotes the angle of depression of the tangent and s is the arc length, (10.1) can be written

$$\frac{\mathrm{d}\alpha}{\mathrm{d}s} = -y + \text{constant.} \tag{10.3}$$

We have also

$$\frac{\mathrm{d}y}{\mathrm{d}s} = -\sin\alpha, \tag{10.4}$$

so that on eliminating y we have

$$\frac{\mathrm{d}^2\alpha}{\mathrm{d}s^2} = \sin\alpha. \tag{10.5}$$

On multiplying by $\mathrm{d}\alpha/\mathrm{d}s$ and integrating with respect to s we obtain

$$\left(\frac{\mathrm{d}\alpha}{\mathrm{d}s}\right)^2 = \kappa_0^2 + 4\sin^2\tfrac{1}{2}\alpha, \tag{10.6}$$

where κ_0 denotes the curvature at the wave crest $\alpha = 0$, $y = 0$. Writing now $\tfrac{1}{2}\alpha = \beta$ and $\tfrac{1}{2}\kappa_0 = \boldsymbol{k}$ we obtain

$$s = \int_0^\beta \frac{\mathrm{d}\beta}{(\boldsymbol{k}^2 + \sin^2\beta)^{\frac{1}{2}}} \tag{10.7}$$

and the displacements x, y from the crest are given by

$$x = \int_0^s \cos\alpha\,\mathrm{d}s = \int_0^{\frac{1}{2}\alpha} \frac{\cos 2\beta}{(\boldsymbol{k}^2 + \sin^2\beta)^{\frac{1}{2}}}\,\mathrm{d}\beta, \tag{10.8}$$

$$|y| = \int_0^s \sin\alpha\,\mathrm{d}s = 2[(\boldsymbol{k}^2 + \sin^2\beta)^{\frac{1}{2}} - \boldsymbol{k}]. \tag{10.9}$$

Clearly (10.7) and (10.8) can be expressed in terms of the standard elliptic integrals E, F and K (see Abramowitz & Stegun 1965) by writing

$$m = \frac{1}{\boldsymbol{k}^2 + 1} = \sin^2\theta, \qquad \gamma = \tfrac{1}{2}\pi - \beta, \tag{10.10}$$

giving

$$s = m^{\frac{1}{2}}[\mathrm{K}(m) - \mathrm{F}(\gamma\,|\,\theta)] \tag{10.11}$$

and

$$x = (1 + \tfrac{1}{2}\kappa_0^2)\,s - 2m^{-\frac{1}{2}}[\mathrm{E}(m) - \mathrm{E}(\gamma\,|\,\theta)]. \tag{10.12}$$

Also

$$|y| = (\kappa_0^2 + 4\sin^2\tfrac{1}{2}\alpha)^{\frac{1}{2}} - \kappa_0, \tag{10.13}$$

and

$$\kappa = (\kappa_0^2 + 4\sin^2\tfrac{1}{2}\alpha)^{\frac{1}{2}}. \tag{10.14}$$
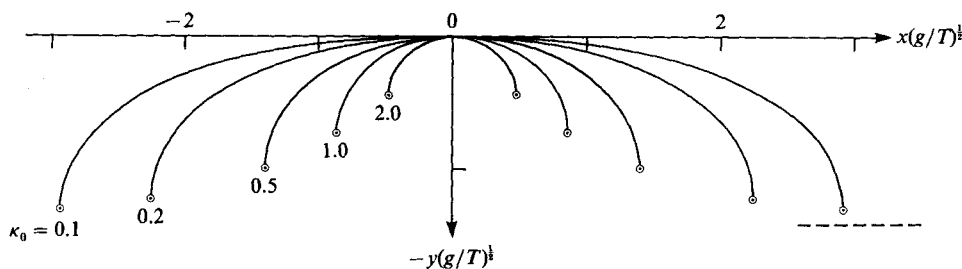
M. S. Longuet-Higgins

FIGURE 10. Solutions to the static equation (10.6) for different values of the initial curvature κ_0.

Some solutions for given values of κ_0 are shown in figure 10. When $\alpha = \frac{1}{2}\pi$, that is, the tangent to the surface profile is vertical, the value y_1 of y from (10.13) is given by

$$|y_1| = (\kappa_0^2 + 2)^{\frac{1}{2}} - \kappa_0. \qquad (10.15)$$

So the depth of this point below the wave crest is always finite, no matter how small the initial curvature. From (10.14) the curvature κ_1 at $\alpha = \frac{1}{2}\pi$ is given by

$$\kappa_1 = (\kappa_0^2 + 2)^{\frac{1}{2}}, \qquad (10.16)$$

which is also finite. The physical explanation is clear. Equations (10.3) and (10.4) are precisely the same as for the surface of a small pool of liquid resting on a plane surface (in two dimensions only). We have simply considered the case when the boundary condition at the plane surface is that the tangent to the liquid be vertical.

In the limit when $\kappa_0 \to \infty$ then $k = \frac{1}{2}\kappa_0$ becomes large and $m \to 0$ so we have

$$|y_1| \sim 1/\kappa_0, \qquad \kappa_1 \sim \kappa_0. \qquad (10.17)$$

The wave profile becomes the arc of a circle, approximating a pure capillary wave. In that case

$$|y_1|/x_1 \to 1. \qquad (10.18)$$

On the other hand when $\kappa_0 \to 0$ then from the asymptotic developments of $\mathrm{E}(\gamma\,|\,\theta)$ and $\mathrm{F}(\gamma\,|\,\theta)$ for small k (see Byrd & Freedman 1971, p. 300) we find that both

$$s_1 = m^{\frac{1}{2}}[\mathrm{K}(m) - \mathrm{F}(\tfrac{1}{4}\pi\,|\,\theta)] \qquad (10.19)$$

and $\qquad\qquad x_1 = (1 + \tfrac{1}{2}\kappa_0^2)\,s_1 - 2m^{-\frac{1}{2}}[\mathrm{E}(m) - \mathrm{E}(\tfrac{1}{4}\pi\,|\,\theta)] \qquad (10.20)$

tend to infinity like $\ln(1/\kappa_0)$. Hence the wavelength

$$L = 2x_1 \qquad (10.21)$$

also tends to infinity, while the wavenumber

$$\pi/x_1 = k = K^{\frac{1}{2}} \qquad (10.22)$$

(in these units) tends to zero. On the other hand we see from (10.15) and (10.16) that in the limit $\kappa_0 \to 0$ we have $|y_1| \to \sqrt{2}$ and $\kappa_1 \to \sqrt{2}$, which are finite. The limiting value of y_1 is shown in figure 10 by the broken horizontal line.

To test the validity of the approximation (10.5) we have plotted in figure 11 the ratio y_1/x_1 as given by equations (10.15) and (10.19) (full curve). In the same diagram are shown the ratios for $K = \infty$, 10, 5 and 1, the first from Crapper's (1957) exact solution, and the others from Hogan's (1980) accurate numerical calculations. In each case the agreement is remarkably close, the error being less than 4%.
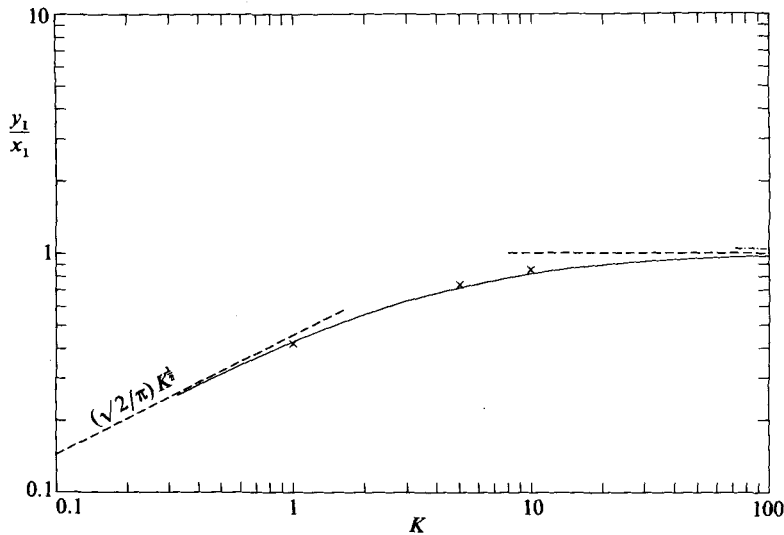
FIGURE 11. The ratio y_1/x_1 as a function of K. The full curve represents the approximate solution (10.15) and (10.20). Crosses represent the full numerical calculations of Hogan (1980).

11. The complete surface profile

To complete the surface profile, we may join the approximate solution for the 'bubble' (in which gravity is neglected and there is a balance between $T\kappa$ and $\frac{1}{2}q^2$) to the approximate solution for the wave crest (in which $\frac{1}{2}q^2$ is neglected and there is a balance between $T\kappa$ and gy) by requiring that the curvature at the top of the bubble, where the solutions meet, be continuous.

As a first check on the approximation we note that the total height H of the wave must equal $(|y_1| + h)$ and hence if L is the wavelength

$$\frac{H}{L} = \frac{|y_1| + h}{2x_1} = \frac{1}{2}\left(\frac{|y_1|}{x_1} + \frac{\kappa_1 h}{\kappa_1 x_1}\right), \qquad (11.1)$$

where κ_1 is the curvature at the 'neck' of the bubble. Now, in the bubble solution of §5 (see also figure 9) we find

$$2\kappa_1/k_{\text{cap}} = 0.5173 \qquad (11.2)$$

and

$$hk_{\text{cap}}/2 = 1.3318, \qquad (11.3)$$

giving

$$\kappa_1 h = 0.3445 \qquad (11.4)$$

independently of the scale. Thus (11.1) may be written

$$H/L = 0.5|y_1|/x_1 + 0.17224/\kappa_1 x_1, \qquad (11.5)$$

where x_1, y_1 and κ_1 are given by equations (10.15), (10.16) and (10.19). In figure 12 we show H/L as a function of $K_1 = (\pi/x_1)^2$. In the same figure are plotted the values computed by Schwartz & Vanden-Broeck (1979, table 3) and by Hogan (1980). The agreement is encouraging.

The area of the limiting bubble in figure 9 is easily found to be 0.032324. In dimensional units the corresponding area is

$$\Omega = 0.03232(2/k_{\text{cap}})^2 = 0.008655\kappa_1^{-2}. \qquad (11.6)$$
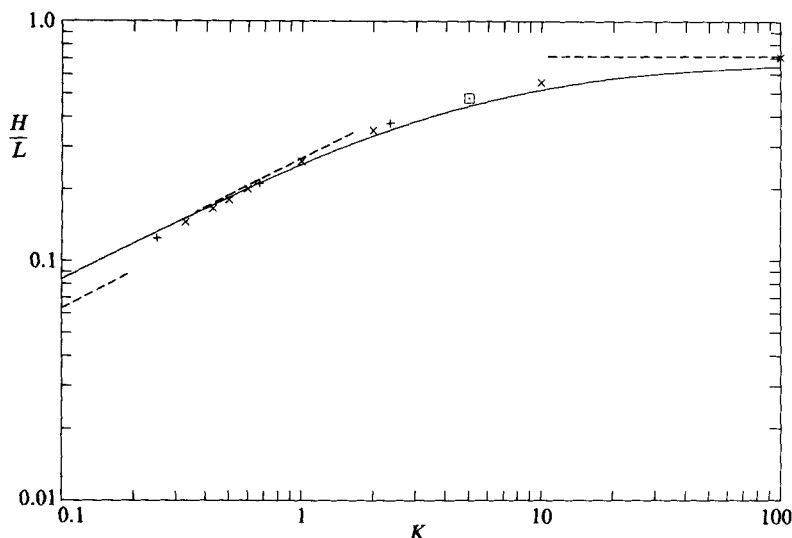
FIGURE 12. The wave steepness H/L as a function of K. The full curve represents the static approximation. Plotted points represent calculations: $\times$, Schwartz & Vanden-Broeck (1979); $\boxdot$, Hogan (1980); $+$, Chen & Saffman (1980). The upper dashed lines represent asymptotes derived from §12. The lower dashed line on the left corresponds to equation (14.12).

This is the same as for a circle of radius

$$a = (\Omega/\pi)^{\frac{1}{2}} = 0.0525\kappa_1^{-1}. \tag{11.7}$$

The circulation Γ_1 round the bubble in figure 9 is 2.0829. Thus in dimensional units we have

$$\Gamma_1 = 2.0829(2c/k_{\text{cap}}) = 1.5689(T/\kappa_1)^{\frac{1}{2}} \tag{11.8}$$

(see equations (12.10) and (12.11)).

12. A solitary wave on deep water?

The results of the two previous Sections strongly suggest the existence, as $K \to 0$, of a solitary wave of Type 1, that is a capillary–gravity wave of finite amplitude in deep water. For waves of limiting steepness, the profile of the wave crest would be given approximately by the solution to (10.6) in the limit $\kappa_0 \to 0$, that is

$$\frac{\mathrm{d}\alpha}{\mathrm{d}s} = -2\sin\tfrac{1}{2}\alpha. \tag{12.1}$$

On moving the origins to the point (x_1, y_1) where $\alpha = \tfrac{1}{2}\pi$ and denoting the corresponding coordinates by primes we have

$$(g/T)^{\frac{1}{2}}s' = \int_\alpha^{\frac{1}{2}\pi} \frac{\mathrm{d}\alpha}{2\sin\tfrac{1}{2}\alpha} = \ln\cot\tfrac{1}{4}\alpha - C, \tag{12.2}$$

where $\qquad\qquad\qquad C = \ln\cot\tfrac{1}{8}\pi = 0.8814.$ $\qquad\qquad\qquad$ (12.3)

Similarly
$$(g/T)^{\frac{1}{2}} x' = \int_\alpha^{\frac{1}{2}\pi} \frac{\cos\alpha}{2\sin\frac{1}{2}\alpha} \, d\alpha = (g/T)^{\frac{1}{2}} s' - 2(\cos\tfrac{1}{2}\alpha - \cos\tfrac{1}{8}\pi) \tag{12.4}$$

$$-(g/T)^{\frac{1}{2}} y' = \int_\alpha^{\frac{1}{2}\pi} \frac{\sin\alpha}{2\sin\frac{1}{2}\alpha} \, d\alpha = \tfrac{1}{2}(\sin\tfrac{1}{2}\alpha - \sin\tfrac{1}{8}\pi) \tag{12.5}$$

and
$$(T/g)^{\frac{1}{2}} \kappa = 2\sin\tfrac{1}{2}\alpha. \tag{12.6}$$

When $\alpha = \frac{1}{2}\pi$ the curvature κ_1 is
$$\kappa_1 = (2g/T)^{\frac{1}{2}}. \tag{12.7}$$

Below the neck of the bubble the flow is given approximately by
$$zk_2/2 = wk_2/2c_2 - \tan(wk_2/2c_2), \tag{12.8}$$

where k_2 is the wavenumber of the complete capillary–wave solution and c_2 is its phase speed. From (5.8) we have
$$c_2^2 = \frac{1-A^2}{1+A^2} k_2 T, \tag{12.9}$$

with $A = 0.455$, hence
$$c_2 = 0.8105(k_2 T)^{\frac{1}{2}}. \tag{12.10}$$

k_2 is determined by the curvature at the neck of the bubble. On equating this to κ_1 we have
$$k_2 = 2\kappa_1/0.5173 = 3.8661\kappa_1 \tag{12.11}$$

from (12.7). If κ_1 is given by (12.7) then
$$k_2 = 5.467(g/T)^{\frac{1}{2}}. \tag{12.12}$$

13. The phase speed: a vortex approximation

To determine the phase speed it is necessary only to know the particle velocity in the far field. For, in deep water, the stream velocity at infinite depths tends to minus the phase speed c. Now in a periodic wave of limiting steepness it is reasonable to compare the far-field flow with that from an array of equal vortices in a uniform stream U (see figure 13), each vortex being situated near a point $z = mL$, $m = 0, \pm 1, \pm 2, \dots$. If Γ denotes the circulation in each vortex, the whole array of vortices induces a horizontal velocity $\pm \Gamma/2L$ at points far below and above the level $y = 0$ respectively. Hence we shall have
$$c = U + \Gamma/2L. \tag{13.1}$$

What should be the appropriate values of U and Γ? We saw that in the case of a pure capillary wave ($K = \infty$) the velocity in the crest of the wave was very small, so that in that case
$$U_{\text{cap}} - \Gamma_{\text{cap}}/2L_{\text{cap}} = 0, \tag{13.2}$$

very nearly. From (13.1) and (13.2) it follows that
$$U_{\text{cap}} = \tfrac{1}{2} c_{\text{cap}}, \qquad \Gamma_{\text{cap}} = L_{\text{cap}} c_{\text{cap}}, \tag{13.3}$$

where the suffix 'cap' refers to pure capillary waves. Hence
$$\Gamma_{\text{cap}} = 2\pi c_{\text{cap}}/k_{\text{cap}}, \tag{13.4}$$

the speed c_{cap} being given by equation (12.10), that is
$$c_{\text{cap}} = 0.8105(k_{\text{cap}} T)^{\frac{1}{2}}. \tag{13.5}$$
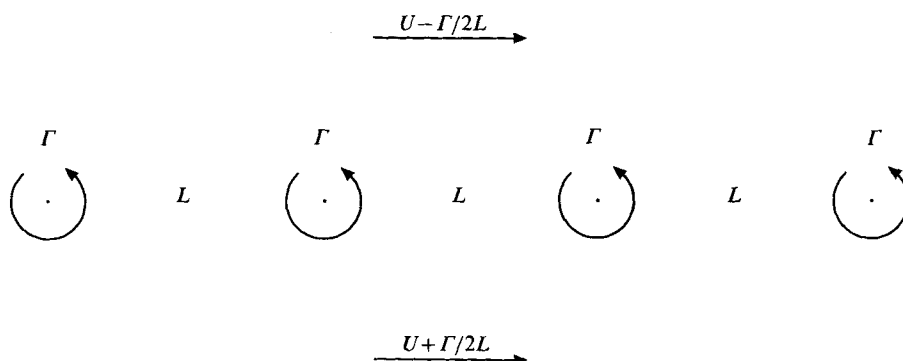
M. S. Longuet-Higgins

FIGURE 13. A vortex approximation for the far-field flow in a limiting capillary–gravity wave.

Consider now capillary–gravity waves of any arbitrary length L. Let us assume that the values of U and Γ are scaled according to the curvature at the neck of the bubble so

$$U = \tfrac{1}{2}c_2, \qquad \Gamma = 2\pi c_2/k_2, \tag{13.6}$$

where c_2 and k_2 are given by (12.10) and (12.12). Then from (13.1) we have

$$c = \tfrac{1}{2}c_2 + \frac{1}{4\pi}\,\Gamma k, \tag{13.7}$$

where

$$k = 2\pi/L = K^{\frac{1}{2}}(g/T)^{\frac{1}{2}}. \tag{13.8}$$

From (13.6) and (13.7) it follows that

$$c = \tfrac{1}{2}c_2(1 + k/k_2) \tag{13.9}$$

and hence

$$c/(gT)^{\frac{1}{4}} = 0.948 + 0.173K^{\frac{1}{2}}. \tag{13.10}$$

In the special case of solitary waves $(K \to 0)$ the influence of the vortices on the far-field velocity tends to zero, and we find

$$c = 0.948(gT)^{\frac{1}{4}}. \tag{13.11}$$

This compares with the value

$$c = 0.923(gT)^{\frac{1}{4}} \tag{13.12}$$

found by Chen & Saffman (1980) in the case $K = 0.042$, their longest wave (see table 3).

In figure 14 are plotted the approximate formula (13.10) (full curve) together with the numerical values of $c/(gT)^{\frac{1}{4}}$ inferred from the work of Schwartz & Vanden-Broeck (1979) and Chen & Saffman (1980); see tables 2 and 3 respectively. The argument is remarkably close.

Note that it is not necessary for the equivalent circulation Γ to be the same as that around the 'bubble', as in (11.8). That equation refers only to the near-field flow. Up to the point of contact, there is in fact no vorticity within the fluid itself.
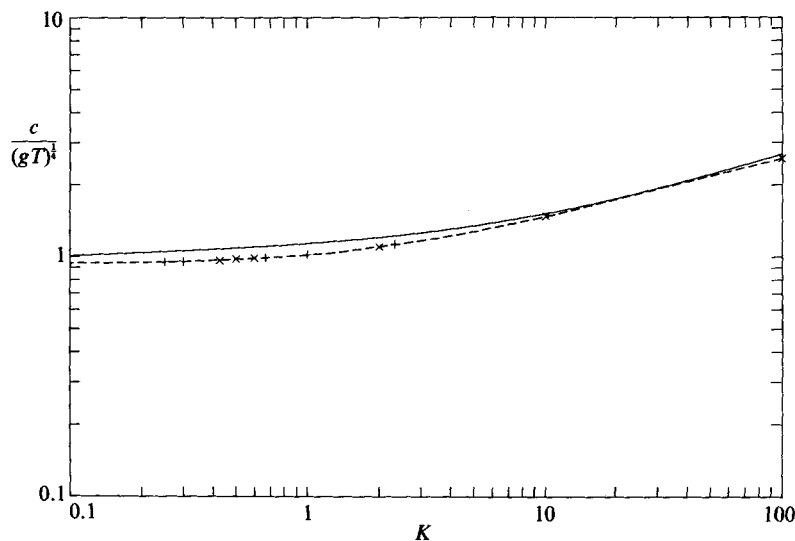
FIGURE 14. The dimensionless phase speed $c/(gT)^{\frac{1}{4}}$ in a capillary–gravity wave of limiting steepness, as a function of K. Full curve represents the vortex approximation; plotted points fully calculated values: ×, Schwartz & Vanden-Broeck (1979); +, Chen & Saffman (1980).

K	H/L	$\mu \equiv c^2 k/g$	$c/(gT)^{\frac{1}{4}}$
1000	0.727	658.0	4.561
100	.703	66.1	2.57
10	.556	6.97	1.48
2	.349	1.69	1.09
1	.257	1.02	1.01
0.6	.198	0.74	0.98
0.5	.179	0.66	0.97
0.43	.165	0.60	0.96
0.33	.14	0.4	1.

TABLE 2. Parameters of limiting capillary–gravity waves of Type 1, as calculated by Schwartz & Vanden-Broeck (1979)

K	H/L	$c(k/g)^{\frac{1}{2}}$	$c/(gT)^{\frac{1}{4}}$
2.333	—	1.3843	1.120
0.666	—	0.8865	0.981
0.3	0.1372	0.7038	0.951
0.25	—	0.6677	0.944
0.042	—	0.4178	0.923

TABLE 3. Parameters of limiting capillary–gravity waves of Type 1 as calculated by Chen & Saffman (1980)

14. The tails of the solitary wave

In accurate calculations of the surface profiles at values of K equal to 0.5 or less one notices a tendency for a shallow dip or hollow to develop near the wave crest (see for example Chen & Saffman (1980), figures 3 and 8, or Hogan (1981), figure 4). This

resembles the 'dimple' in the profile of a weakly nonlinear ripple, noted first by Wilton (1915) at certain critical wavenumbers, and now usually attributed to resonances between the fundamental wavelength and some higher harmonic which travels at the same speed. For the longer waves, however, the speed c of the complete wave can be much slower than the minimum phase speed $c_{\min} = (4gT)^{\frac{1}{4}}$ for free capillary–gravity waves of low steepness. Hence a second or higher harmonic would not resonate; the extra displacements must be mainly forced.

We shall show that in the steep waves under discussion the effect can be attributed to the non-zero velocity in the far field, which so far we have neglected. Consider the case of the solitary wave. Assuming the particle velocity in the far field consists of a uniform stream $U = \frac{1}{2}c_2$ together with a vortex of strength $\Gamma/2\pi$ at $z = 0$ then the local particle speed will be given by

$$q^2 = |\tfrac{1}{2}c_2 + \Gamma/(2\pi i z)|^2. \tag{14.1}$$

For large values of x we shall have asymptotically

$$q^2 = \tfrac{1}{4}c_2^2 + \frac{\Gamma}{2\pi}\left(\frac{\Gamma}{2\pi} - c_2 y_\infty\right)x^{-2} \tag{14.2}$$

to order x^{-2}, where y_∞ denotes the limiting value of y. The boundary condition (2.4) then becomes

$$y + (T/g)\kappa = y_\infty + Bx^{-2}, \tag{14.3}$$

where

$$B = \frac{\Gamma}{4\pi g}\left(cy_\infty - \frac{\Gamma}{2\pi}\right). \tag{14.4}$$

For small slopes, the curvature κ is approximately $-\mathrm{d}^2y/\mathrm{d}x^2$, so for large x the appropriate solution to (14.3) tending to y_∞ as $x \to \infty$ is, to lowest order in $1/x$,

$$y = y_\infty + Bx^{-2} + C\,\mathrm{e}^{-(g/T)^{\frac{1}{2}}x} \tag{14.5}$$

where C is a constant to be determined. (We note that as $x \to \infty$ the exponential term is dominated by the term in x^{-2}).

To determine the constant C, the solution (14.7) may be joined to the rest of the profile at some point $x = x_M$, say. We have no expression for the velocity field at intermediate distances other than the static approximation $q = 0$. So in order to preserve continuity in the curvature κ we interpolate q^2 by the expression

$$q^2 \doteq (1 - x_M^4/x^4)\,|\tfrac{1}{2}c_2 + \Gamma/(2i\pi z)|^2, \tag{14.6}$$

which vanishes at the matching point x_M and also preserves the asymptotic form (14.2) of q^2 as $x \to \infty$.

To determine y_∞ we write (14.3) as

$$y + (T/g)\kappa + q^2/2g = y_\infty + c_2^2/8g \tag{14.7}$$

so that setting $q = 0$ we have

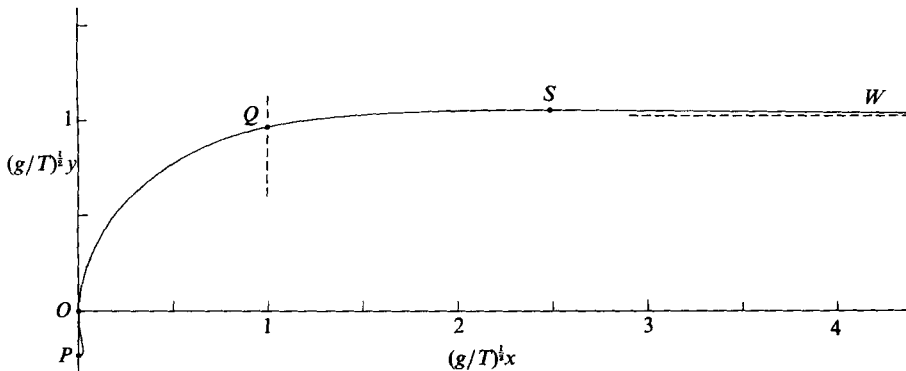$$y_\infty + c_2^2/8g = y_M + (T/g)\kappa_M = (T/g)\kappa_1. \tag{14.8}$$

FIGURE 15. Approximate profile of the solitary capillary–gravity wave. OP: capillary approximation; OQ: static approximation; QSW: vortex approximation.

In practice, the simplest way to perform the joining is to integrate the equations

$$\left.\begin{array}{l} \mathrm{d}x/\mathrm{d}s = \cos\alpha, \\ \mathrm{d}y/\mathrm{d}s = \sin\alpha, \\ \mathrm{d}\alpha/\mathrm{d}s = y + \tfrac{1}{2}q^2 - (T/g)\,\kappa_1 \end{array}\right\} \tag{14.9}$$

forward from $s = 0$ where $x = 0$, $y = 0$, $\alpha = \tfrac{1}{2}\pi$ taking

$$q^2 = \left\{\begin{array}{ll} 0, & |x| < x_{\mathrm{M}}, \\ (14.6), & |x| > x_{\mathrm{M}}. \end{array}\right\} \tag{14.10}$$

The curvature κ at $\alpha = \tfrac{1}{2}\pi$ may be taken initially as some large value, and then gradually decreased until the solution becomes a solitary wave, that is to say $x \to \infty$ as $\alpha \to 0$, within practical limits.

If we choose $x_{\mathrm{M}} = 1$ we obtain the profile shown in figure 15. This corresponds to an initial curvature

$$\kappa_1 = 1.495(g/T)^{\frac{1}{2}}, \tag{14.11}$$

only slightly greater than the value (12.7) for the static approximation. In the present case the surface rises to

$$y_{\max} = 1.050(T/g)^{\frac{1}{2}} \quad \text{at } x = 2.485(T/g)^{\frac{1}{2}}$$

before falling gradually towards $y_\infty = 1.020(T/g)^{\frac{1}{2}}$ as $x \to \infty$. The matching point is at $x_{\mathrm{M}} = 0.7680(T/g)^{\frac{1}{2}}$.

For comparison with computed values we show in table 4 some data from Chen & Saffman (1980) and Hogan (1981). The 'dimple' at the crest seems to appear at first between $K = 0.666$ and $K = 0.5$. As K decreases further, the position x of the maximum elevation seems to tend towards $x = 3.12(T/g)^{\frac{1}{2}}$, compared with our (approximate) limiting value $3.14(T/g)^{\frac{1}{2}}$. The depth Δy of the dimple below the highest point of the profile is difficult to determine from Chen & Saffman's figure 8. At $K = 0.042$, δ appears to be about $0.087(T/g)^{\frac{1}{2}}$.

The effect of taking different values for the matching point x_{M} is shown in table 5. The range $0.8 < x_{\mathrm{M}} < 1.5$ effectively covers the likely values of $x_{\max}$ and Δy. Over this range, however, κ_1 varies only between 1.517 and 1.458.

K	kx	$(g/T)^{\frac{1}{2}}x$	$k(y_{max}-y_{L/2})$	$(g/T)^{\frac{1}{2}}(y_{max}-y_{L/2})$
∞	π	∞	0	0
2.333	π	6.508	0	0
0.666	π	3.850	0	0
†0.5	2.276	3.219	0.0227	0.0321
0.3	1.74	3.18	0.013	0.023
0.250	1.56	3.12	0.032	0.064
0.042	0.64	3.12	0.018	0.087

† Hogan (1981), figure 4.

TABLE 4. Parameters of the dimple at the crest of limiting capillary–gravity waves, from Chen & Saffman (1980), figures 3 and 8

x_M	x_{max}	y_{max}	y_∞	Δy	κ_1
0.8	3.251	1.053	1.035	.018	1.517
1.0	2.485	1.050	1.020	.030	1.495
1.5	1.797	1.104	0.995	.109	1.458

TABLE 5. Parameters of the approximate solitary wave profile. The unit length is $(T/g)^{\frac{1}{2}}$.

For the sake of discussion we may take the value (14.11) corresponding to $x_M = 1$. Then the vertical extent h of the bubble, from (11.4), is $0.230(T/g)^{\frac{1}{2}}$. Hence

$$\frac{y_\infty + h}{L} = \frac{k(y_\infty + h)}{2\pi} = 0.199(T/g)^{\frac{1}{2}}. \tag{14.12}$$

This asymptote is shown in figure 12 by the lower dashed line on the left. The plotted points ($+$) from Chen & Saffman (1980) have been estimated, to graphical accuracy, from their figure 8. Their value of $(y_{L/2}-y_0)/L$ when $K = 0.042$ (not shown here) is 0.049, compared to 0.041 from (14.12). Hence it appears that the computed values approach the asymptote in figure 12.

In this section we have shown, at least qualitatively, that the effect of adding a velocity field to the static approximation is to *reduce* the height of the crest in a solitary wave, since the particle speed q reaches its maximum value $\frac{1}{2}c_2$ at large distances. With waves of finite length, however, this is not necessarily true. For example in very short waves we have seen that q is a minimum at the crest. For large K, therefore, we expect that the effect of the velocity field will be to *increase* the estimated wave steepness. This indeed is seen in figure 12, when $K > 1$.

15. Bubble diameters

Since the curvature κ_1 is a monotonically decreasing function of K, equation (12.7) represents the minimum curvature: $\kappa_{1\,min}$. Hence (11.7) represents the maximum diameter of the 'bubble' in a two-dimensional situation. If such a cylindrical bubble is indeed formed it will quickly break up into spherical bubbles, whose volume will depend on the wavelength λ of the initial longitudinal instability. Chandrasekhar (1961) gives for the fastest-growing capillary instability of a hollow jet $2\pi a/\lambda = 0.484$, hence $\lambda = 6.49 \times 2a$. However, owing to the initially very distorted shape of the bubble cross-section, this may be an overestimate. Chandrasekhar neglects the
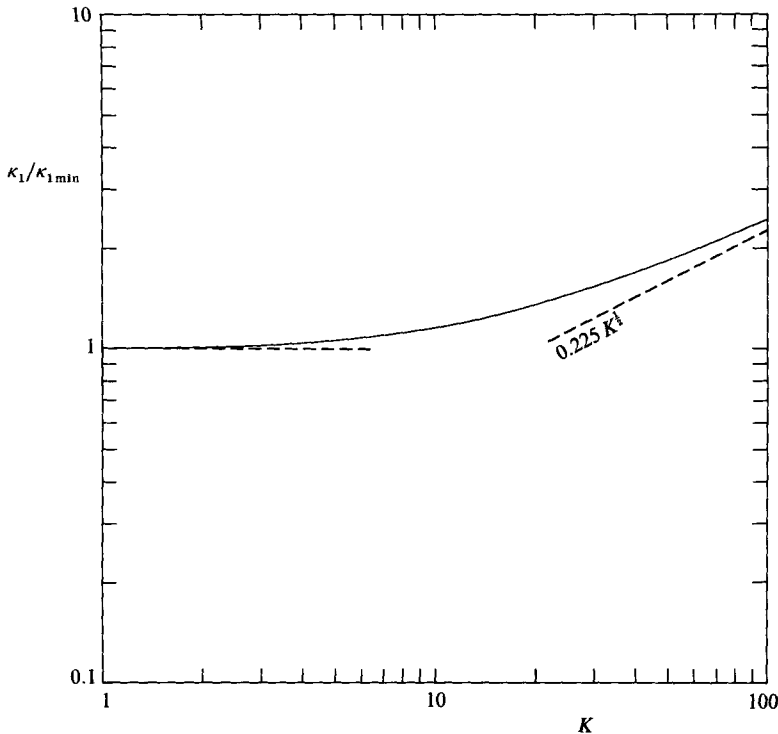
FIGURE 16. The ratio $\kappa_1/\kappa_{1\max}$ as a function of K.

rotation of the jet. Assuming the wavelength of the most unstable perturbation to be of order $4\pi a$, the volume of air enclosed by a single bubble will be of order

$$V = 4\pi^2 a^3, \tag{15.1}$$

where a is given by (11.7). The diameter $d_{\max}$ of a spherical bubble with such a volume will be

$$d_{\max} = (6V/\pi)^{\frac{1}{3}} = 4.22a = 0.221\kappa_1^{-1} = 0.146(T/g)^{\frac{1}{2}}, \tag{15.2}$$

which is about 0.40 mm.

Shorter waves would produce bubbles with a diameter d inversely proportional to the curvature κ_1; thus

$$d/d_{\max} = (\kappa_1/\kappa_{\max})^{-1}. \tag{15.3}$$

This ratio is shown in figure 16 as a function of K.

In the experiments of Schooley (1958) the steepest gravity waves in his figures 6 and 7, for example, have wavelengths of about 7 cm, corresponding to $K \doteq 6$. From figure 16 we see that this implies a ratio $\kappa_1/\kappa_{1\min}$ of about 1.08. Hence we would expect $d = 0.37$ mm approximately. One cannot be sure that the bubbles visible in his photographs are indeed due to these particular waves. Nevertheless it is interesting that the largest bubbles in his figure 7 have diameters of about 0.3 mm, of the same order of magnitude as predicted.

16. Further discussion

We have discussed only limiting capillary–gravity waves of Type 1. The work of Schwartz & Vanden-Broeck (1979), Chen & Saffman (1979, 1980) and others shows the existence, at a given wavelength, of other types of wave which at large steepnesses also develop capillary-type 'pinches' in the wave trough. It should be possible to develop similar approximations for these also, on the basis that they are essentially Type 1 quasi-capillary waves superposed on longer quasi-gravity waves.

We note that the solitary waves postulated in §12 are essentially waves of finite amplitude, and could not exist in a linear theory, where only sinusoidal solutions are possible. In this respect the situation resembles that of the well-known solitary gravity waves in water of finite depth.

In all of the above work we have of course assumed irrotational flow and neglected both viscosity and any elasto-viscous effects due to surface films. Under such conditions the extent of the agreement with observation found in §13 is as good as might be expected, though further experiments and observations are desirable.

In the ocean, a favourable situation for the generation of steep capillary–gravity waves may be in the troughs of long but steep gravity waves. For, the shorter gravity waves tend to be limited by breaking at the long-wave crests, and then to be smoothed out in the troughs by orbital stretching. This may leave a clean slate on which the action of the wind can regenerate capillary waves.

One interesting effect will arise from the vorticity injected into the flow because of the circulation Γ_1 around the bubbles. Initially this will generate a kind of irrotational shear. A row of bubbles spaced at regular distances D in the horizontal direction will induce a surface current of strength equal to Γ_1/D. Since there is little friction inside the bubbles the surface current is carried, so to speak, on roller bearings. A rate of production of N bubbles per unit time and per unit horizontal distance would be accompanied by a horizontal acceleration of the surface equal to $N\Gamma_1$. However, this will be balanced by an actual viscous dissipation of vorticity. With further data on bubble production the calculation might be usefully elaborated.

17. Conclusions

We have shown that in steep capillary–gravity waves in a perfect fluid:

(1) The shape of the 'bubble' which forms in the wave trough is hardly affected at all by gravity; its profile is almost exactly as given by the solution for pure capillary waves.

(2) The size of the 'bubble' is determined by the radius of curvature at the bubble neck, and has a finite upper bound.

(3) The form of the wave crest above the bubble is given to fair accuracy by a static approximation, in which gravity is balanced by capillarity and the particle velocity is neglected. This static approximation indicates the existence of a solitary capillary–gravity wave on deep water, in which, as the wavelength goes to infinity (on a scale of $(T/g)^{\frac{1}{2}}$), the depth of the wave trough remains finite.

(4) The effect of the particle velocity on the profile of long waves ($K \ll 1$) is to produce a shallow depression, or dimple in the crest. For very short waves ($K \gg 1$) this effect is reversed, and there is a gain in crest height.

(5) The profile of the solitary wave has been determined approximately. The corresponding bubble, formed after collapse of the surface, has a diameter of about

0.37 mm, which is not inconsistent with the laboratory observations by Schooley (1958).

(6) Some simple elementary solutions for pure capillary flows have been brought to light, which could be useful in other contexts.

We have considered only steady motions. The fully time-dependent problem, including the compressibility of the water and the generation of an acoustical signal, will be considered in a subsequent paper.

Note added in proof. Since this paper was accepted for publication, the author has carried out accurate numerical calculations providing strong evidence for the existence of a whole family of capillary-gravity waves of solitary type on deep water. The crest-to-trough wave heights lie within a certain range. The family includes as a special case a wave of limiting amplitude resembling that shown in figure 15 above.

REFERENCES

ABRAMOWITZ, M. & STEGUN, I. A. (eds) 1965 *Handbook of Mathematical Functions.* Dover. 1046 pp.

BYRD, P. F. & FRIEDMAN, M. D. 1971 *Handbook of Elliptic Integrals for Engineers and Scientists*, 2nd edn. Springer. 358 pp.

CHANDRASEKHAR, S. 1961 *Hydrodynamic and Hydromagnetic Stability.* Clarendon. 654 pp.

CHEN, B. & SAFFMAN, P. G. 1979 Steady gravity-capillary waves on deep water – I. Weakly nonlinear waves. *Stud. Appl. Math.* **60**, 183–210.

CHEN, B. & SAFFMAN, P. G. 1980 Steady gravity-capillary waves on deep water – II. Numerical results for finite amplitude. *Stud. Appl. Math.* **62**, 95–111.

CRAPPER, G. D. 1957 An exact solution for progressive capillary waves of arbitrary amplitude. *J. Fluid Mech.* **2**, 532–540.

HOGAN, S. J. 1980 Some effects of surface tension on steep water waves. Part 2. *J. Fluid Mech.* **96**, 417–445.

HOGAN, S. J. 1981 Some effects of surface tension on steep water waves. Part 3. *J. Fluid Mech.* **110**, 381–410.

KINNERSLEY, W. 1976 Exact large amplitude capillary waves on sheets of fluid. *J. Fluid Mech.* **77**, 229–241.

SCHOOLEY, A. H. 1958 Profiles of wind-created water waves in the capillary-gravity transition region. *J. Mar. Res.* **16**, 100–108.

SCHWARTZ, L. W. & VANDEN-BROECK, J.-M. 1979 Numerical solution of the exact equations for capillary-gravity waves. *J. Fluid Mech.* **95**, 119–139.

TAYLOR, G. I. 1959 The dynamics of thin sheets of fluid. II. Waves on fluid sheets. *Proc. R. Soc. Lond.* A **253**, 296–312.

VANDEN-BROECK, J.-M. & KELLER, J. B. 1980 A new family of capillary waves. *J. Fluid Mech.* **98**, 161–169.

WILTON, J. R. 1915 On ripples. *Phil. Mag.* (6) **29**, 688–700.